ACS Sustainable Chemistry & Engineering

Research Article

pubs.acs.org/journal/ascecg

Performance and Aging of Mn/MnO_2 as an Environmentally Friendly Energetic Time Delay Composition

Eric J. Miklaszewski,[†] Anthony P. Shaw,[‡] Jay C. Poret,[‡] Steven F. Son,[†] and Lori J. Groven*,[†,§]

[†] School of Mechanical Engineering, Purdue University, West Lafayette, Indiana 47907, United States

[‡] Pyrotechnics Technology and Prototyping Division, U.S. Army RDECOM-ARDEC, Picatinny Arsenal, New Jersey 07806, United States

[§] Department of Chemical and Biological Engineering, South Dakota School of Mines and Technology, Rapid City, South Dakota 57701, United States

Supporting Information

ABSTRACT: The Mn/MnO_2 reactive system was investigated as a suitable replacement for the traditional $W/BaCrO_4/KClO_4$/diatomaceous earth delay composition. The delay performance, ignition sensitivity, and aging characteristics were examined in aluminum microchannels similar in diameter to common delay housings (4.7 mm). Stoichiometries with measured combustion temperatures between 1358 and 2113 K were self-sustaining with combustion velocities ranging from 2.4 to 7.3 mm s^{-1}. The Mn/MnO_2 system produced less gas than $W/BaCrO_4/KClO_4$/diatomaceous earth compositions allowing consideration for use in sealed delay housings. Accelerated aging at 70 °C and 30% relative humidity for 8 weeks resulted in no measurable loss of performance. Safety characterization showed that this composition is not sensitive to ignition by friction or electrostatic stimuli. The combustion products (as determined by X-ray diffraction) appear to be benign based on current regulations. Therefore, the Mn/MnO_2 system appears to be a suitable low gas-producing, nonsensitive, less toxic delay composition with good longevity.

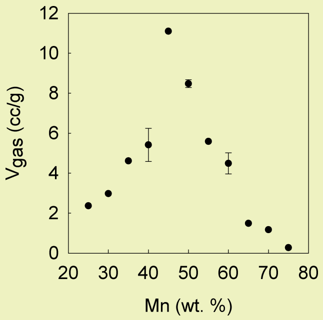

KEYWORDS: *Pyrotechnic, Environmentally benign, Microchannel combustion, Pyrotechnic time delays, Manganese, Manganese dioxide, Aging*

INTRODUCTION

Combustion of pyrotechnic time delay compositions are engineered to provide a repeatable time increment in the firing train of munitions. These mixtures generally consist of metal fuel (W, Mn, etc.) and various oxidizers (chromates, perchlorates) as well as diluents. Traditional pyrotechnic delay compositions such as $W/BaCrO_4/KClO_4$/diatomaceous earth and $Mn/BaCrO_4/PbCrO_4$ have been used since the 1950s due to their dependability and wide range of combustion velocities (0.6−150 mm s^{-1}).[1−6] Additional requirements for delay compositions include low gas production, compliance with evolving environmental regulations, low ignition sensitivity to various stimuli (e.g., friction, electrostatic discharge), and long-term storage stability, which motivates the development of new compositions. Several fielded compositions are highly scrutinized due to their environmentally hazardous components (i.e., $BaCrO_4$, $PbCrO_4$, and $KClO_4$).[7−9] Recent efforts have investigated various alternate compositions (e.g., metal/metal oxide, intermetallics, metalloid/metal oxide), which are capable of propagating at rates less than 5 mm s^{-1}. However, they may contain environmentally questionable constituents, have relatively high gas production, or only propagate at low packing densities.[10−15]

Swanepoel et al.[16] investigated the Mn/Bi_2O_3 and Mn/MnO_2 thermite systems and demonstrated combustion velocities in the range of 5−22 mm s^{-1}. However, the Mn used in that study was waste Mn from a local industrial plant, and the delay processing method was quite different than that currently used by many United States delay manufacturers.[16] At very low packing densities, Kappagantula et al.[17] showed that micron and nano-sized Mn/MnO_2 is nearly gasless and exothermic enough to overcome the heat losses associated with borosilicate channels as small as 3 mm. The low gas evolution and previously demonstrated combustion velocities indicate that this system might be an excellent replacement candidate for traditional delay compositions. To accomplish this, a performance evaluation with standard commercially available materials and processing techniques is needed in order for this composition to be fully considered as a replacement time delay composition. The objective of this work was to study Mn/MnO_2 as a pyrotechnic delay composition with detailed combustion velocity experiments, gas production measurements, combustion product analysis, sensitivity testing, and accelerated aging experiments.

Received: March 3, 2014
Revised: April 4, 2014
Published: April 16, 2014

EXPERIMENTAL SECTION

Reactive Compositions. Nominal sizing and vendor information for the powders used in these experiments are summarized in Table 1.

Table 1. Vendor Information of Reactant Powders

powder	nominal particle size	vendor
Bi_2O_3	15.4 μm	Alfa Aesar
$BaCrO_4$	MIL-B-550A, grade A	Hummel Croton
black powder	Class 7, 40−100 mesh	–
diatomaceous earth	15.4 μm	Sigma-Aldrich
Fe_2O_3 (III)	−325 mesh	Firefox Enterprises
$KClO_4$	MIL-P-217A, grade A, Class 4	Hummel Croton
Mn	−325 mesh	Alfa Aesar
MnO_2	−325 mesh	Alfa Aesar
Si	MIL-S-230C, grade 2, Class C	AEE
W	MIL-T-48140, Type 1	AEE
Zr	−325 mesh	Alfa Aesar

Particle size distributions for Mn and MnO_2 were obtained using a Malvern Mastersizer 2000 equipped with a Hydro 2000 μP dispersant unit with ethanol as the dispersant. Figure S1 of the Supporting Information shows the Mn and MnO_2 particle size data.

Mn/MnO_2 compositions were dry mixed in 30 mL HDPE bottles using a Resodyn LabRAM mixer at 80% intensity in 2 min intervals for a total of 6 min. The details of the mixing procedures used for the W/$BaCrO_4$/$KClO_4$/diatomaceous earth, A1A, and Si/Bi_2O_3 compositions are supplied in the Supporting Information.

Combustion Experiments. Microchannels of similar size to a typical fielded delay housing were used for combustion experiments and consisted of 2024 grade T3 aluminum tubes with inner/outer diameters of 4.7/9.3 mm.[12] To achieve the desired packing density in the channels, reactive compositions were pressed to a stop using a Carver 12 ton press. A dwell time of approximately 10 s was used. Approximately 1 mm of igniter composition was pressed on either end of the channel to act as an ignition source and to signal when the reaction reached the end of the microchannel. One igniter used in this study, referred to as A1A, is composed of 65 wt % Zr, 25 wt % Fe_2O_3, and 10 wt % diatomaceous earth. Other igniter systems used were black powder and a mixture of 30 wt % Si and 70 wt % Bi_2O_3. The various microchannel configurations are shown in Figure 1, and the different igniter combinations are summarized in Table 2.

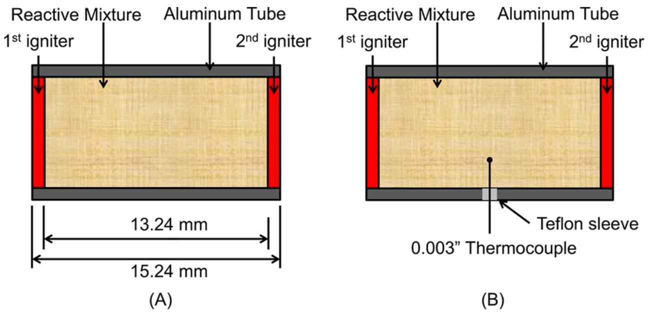

Figure 1. (a) Baseline microchannel configuration. (b) Microchannel with microthermocouple port for combustion temperature measurements.

Table 2. Igniter Configurations

configuration name	1st igniter (input)	2nd igniter (output)
igniter A	A1A	A1A
igniter B	Si/Bi_2O_3 (30/70)	black powder

A 30 gauge electrically heated nichrome wire was used to ignite the first ignition increment. A Sony HandyCam digital video camera was used to record the experiment at 30 frames per second, and the combustion velocity was determined by dividing the length of the microchannel by the time between first light observed on either side of the channel. Temperature profiles of the reacting composition were measured *in situ* by inserting a 0.20 mm B-type thermocouple through a microthermocouple port as displayed in Figure 1b. For near stoichiometric Mn/MnO_2 mixtures, a 0.08 mm C-type thermocouple was used because the peak combustion temperature was found to exceed that of the B-type (temperature maximum of 1973 K).

Gas Generation Measurements. Tap compacted Mn/MnO_2 powder (1.2 ± 0.1 g) was ignited with an electrically heated 30 gauge nichrome wire in air at ambient conditions in an instrumented 151 mL stainless steel constant volume vessel. The internal pressure of the vessel was measured with a Druck PMP 1260 pressure transducer during combustion experiments. The transducer signal was recorded at 100 Hz using a National Instruments SCXI-1300 signal conditioner and a custom LabView program. Gas production was determined from the vessel pressure measurements using eq 1, where ΔP_{comb} is the peak pressure rise due to the combustion event, V_{comb} is the volume of the combustion chamber, P_{amb} is the ambient pressure, and m_{comp} is the mass of the composition reacted. The volume of gas produced by a composition in ambient conditions was approximated by the partial pressure of the combustion gases (0−10 kPa) adiabatically expanded to atmospheric conditions. This approximation assumes the heat losses to the combustion chamber are minimal during combustion (~1 s duration). The gas produced from the reaction is reported in cubic centimeters per gram of reacted mixture (cc g^{-1}).

$$V_{gas}\ (\mathrm{cc\ g^{-1}}) = \frac{\Delta P_{comb} V_{comb}}{P_{amb}} \times \frac{1}{m_{comp}} \qquad (1)$$

Accelerated Aging. An 8 week accelerated aging study was conducted using neat Mn and three different stoichiometries of premixed Mn/MnO_2 according to the aging standard NAVSEAINST 8020.5C.[18] Loose powder samples were stored in open 30 mL LDPE bottles in a Tenney TJR environmental test chamber at 70 ± 1 °C, while a saturated salt bath solution (magnesium chloride hexahydrate) with a humidity feedback controlled water addition maintained the relative humidity at 30 ± 1%. The combustion velocity of the aged powders was evaluated in the previously described experimental combustion setup (4.7 mm Al channels) every 2 weeks. The thermal behavior of unaged and aged Mn was assessed with a TA Instruments Q600 DSC/TGA in 90 μL alumina pans over a range from 200 to 1200 °C at heating rates of 20 °C min^{-1} under Ar/O_2 (80/20 by volume) at a flow rate of 100 mL min^{-1}.

Sensitivity Analysis. Safety characteristics of both igniter compositions and the stoichiometric Mn/MnO_2 composition were evaluated using standard procedures from MIL-STD-1751A.[19] Electrostatic discharge (ESD) sensitivity was assessed using method 1032 (ARDEC). Friction sensitivity was determined using method 1024 (BAM) on a Chilworth machine.

RESULTS AND DISCUSSION

Theoretical and Experimental Combustion Temperatures. In this study, the reaction shown in eq 2 was considered. This reaction proceeds by a series of decompositions from MnO_2 to Mn_2O_3 at approximately 870 K, which then later decomposes to Mn_3O_4 at 1150 K. These decomposition reactions release gaseous O_2 that exothermically reacts with whatever fuel is present (i.e., Mn).[16,20−22] Thermochemical predictions of this reaction were made using Cheetah v6.0[23] at a constant pressure of 1 atm. Figure 2 shows that the predicted adiabatic combustion temperature depends on stoichiometry. As such, the theory from Zeldovitsch et al.[24] predicts that the combustion velocity will also depend on stoichiometry. At stoichiometric conditions (39 wt % Mn), the maximum theoretical adiabatic combustion temperature of 2484 K is predicted. Due to the high heat losses of the small

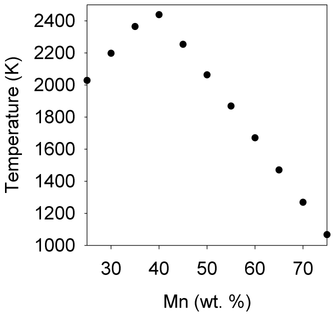

Figure 2. Predicted adiabatic combustion temperature vs Mn content using Cheetah v6.0.

scale of the experiments presented here, adiabatic conditions cannot be assumed. As expected, Figure 3 shows that experimentally measured combustion temperatures vary greatly with stoichiometry. The maximum experimental peak temperature (2113 K) was measured at near-stoichiometric conditions, while the minimum peak temperature (1358 K) was measured for the most fuel-rich mixture (70 wt % Mn). While this temperature is below Merzhanov's prediction that purely condensed phase reactions will not self-propagate below ~1800 K, delay compositions that produce low quantities of gas such as $W/BaCrO_4/KClO_4$/diatomaceous earth and $Mn/BaCrO_4/KClO_4$ are documented to be self-sustaining at much lower temperatures, as low as 1123 K.[4,25]

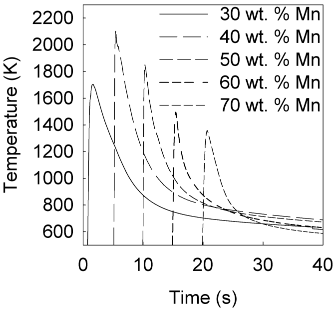

Figure 3. Mn/MnO_2 combustion temperature profiles at various stoichiometries in Al microchannels at 60% TMD. The x-intercept of this data is staggered by 5 s for presentation clarity.

$$x\mathrm{Mn} + y\mathrm{MnO_2} \rightarrow z\mathrm{MnO} + \left(\frac{1}{2}y - \frac{1}{4}z\right)\mathrm{Mn_3O_4} + \left(x - \frac{1}{2}y - \frac{1}{4}z\right)\mathrm{Mn} \qquad (2)$$

Sensitivity and Role of Igniter Type and Stoichiometry. To document delay time performance, a range of stoichiometries were assessed with two different igniter systems. Igniter A (A1A) is an effective igniter due to its high predicted combustion temperature of 3744 K (1 atm) but has been documented to be sensitive to ignition via ESD.[26] Military standard A1A has a documented ESD ignition threshold of 0.05 mJ due to the zirconium powder.[27] A second less sensitive igniter B (Si/Bi_2O_3(30/70)) was also considered even though it has a lower predicted combustion temperature of 2031 K. Electrostatic discharge and friction sensitivity for both igniters is presented in Table 3. Since pyrotechnic compositions are often produced in large quantities, the ignition sensitivity of the Mn/MnO_2 composition to various stimuli must also be known. Near-stoichiometric Mn/MnO_2 (40/60) was found to be insensitive to both ESD and friction stimuli according to MIL-STD-1751A.[19] For comparison, a standard $W/BaCrO_4/KClO_4$/diatomaceous earth composition (32/53/10/5 by wt %) was also found to be insensitive to both ESD and friction stimuli according to MIL-STD-1751A.[19,28]

Table 3. Sensitivity of Compositions to ESD and Friction Stimuli. Nominal Ignition Thresholds Were Determined Using the Bruceton 50% Method as Described in MIL-STD-1751A[19]

composition	ESD threshold (mJ)	friction threshold (N)
A1A (this study)	<0.1	282.5
A1A (MIL-SPEC)[27]	0.05	–
Mn/MnO_2 (40/60)	>250	>353.2
Si/Bi_2O_3 (30/70)	16	>353.2

Figure 4 shows the role stoichiometry has on combustion velocity, with a trend resembling that previously presented by Swanepoel et al.[16] Repeatability was demonstrated with three experiments at 40, 50, and 60 wt % Mn resulting in combustion velocities of 5.99 ± 0.10, 6.62 ± 0.16, and 4.73 ± 0.16 mm s^{-1}, respectively; the reported error is the standard deviation of the velocity measurement. The peak combustion velocity was observed at slightly fuel-rich conditions (45 wt % Mn). Between 40 and 65 wt % Mn, full propagation was observed for both igniters used with little difference in measured combustion velocity. However, for the most fuel-lean or fuel-rich mixtures (30 and 70 wt % Mn), only the hotter igniter (A1A) led to full propagation. Overall, a range of combustion velocities between 2.4 and 7.3 mm s^{-1} was achieved with the Mn/MnO_2 system for mixtures ranging from 30 to 70 wt % Mn. Though the $W/BaCrO_4/KClO_4$/diatomaceous earth delay composition has a larger range of available combustion velocities (0.6−150 mm s^{-1}),[1,5] future work should explore additives to the Mn/MnO_2 system to further tailor the combustion velocity.

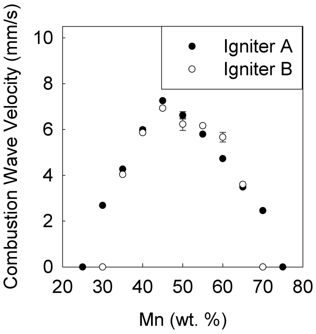

Figure 4. Combustion wave velocity of Mn/MnO_2 as a function of Mn wt % in 4.7 mm Al channels at 60% TMD.

Effect of Stoichiometry on Gas Generation. The measured gas production of Mn/MnO_2 was directly compared to that of the $W/BaCrO_4/KClO_4$/diatomaceous earth system by assessing both in a small constant volume vessel. The gas generation of four different $W/BaCrO_4/KClO_4$/diatomaceous earth compositions was evaluated with three experiments each. Table 4 shows that these compositions produced gas volumes from 15.7 to 29.4 cc g_{mix}^{-1}. Figure 5 shows the gas production volume of Mn/MnO_2 as a function of stoichiometry, and corresponding error bars are shown. Repeatability was assessed with three experiments at 40, 50, and 60 wt % Mn. Similar to

Table 4. Produced Gas Volume of Various W/$BaCrO_4$/$KClO_4$/Diatomaceous Earth Compositions

W/$BaCrO_4$/$KClO_4$/diatomaceous earth (wt %)	V_{gas} (cc/g)
35/50/10/5	19.0 ± 3.1
50/35/10/5	29.4 ± 2.2
50/40/5/5	15.7 ± 2.0
65/25/5/5	18.8 ± 1.4

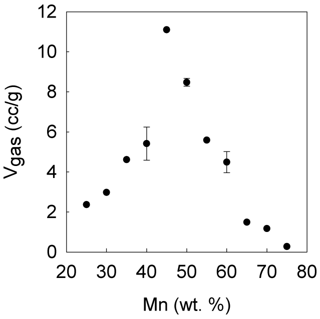

Figure 5. Measured gas volume produced as a function of stoichiometry for Mn/MnO_2.

the combustion velocities, gas production was greatest at 45 and least at 70 wt % Mn. For all stoichiometries, the Mn/MnO_2 system produces less gas (<12 cc g_{mix}^{-1}) than the W/$BaCrO_4$/$KClO_4$/diatomaceous earth compositions, which allows consideration for use in sealed delay housings.

Environmental Assessment of Combustion Products. Ideally, modern delay compositions will not have constituents or combustion products that are hazardous or highly regulated (e.g., $BaCrO_4$, $PbCrO_4$, $KClO_4$, or others). For the W/$BaCrO_4$/$KClO_4$/diatomaceous earth composition, both the reactants and the combustion products can contain toxic chemicals such as $BaCrO_4$.[4] X-ray diffraction analysis of the combustion products for the Mn/MnO_2 system is shown in Figure 6 and indicates a shift in product formation when the stoichiometry is fuel-rich, fuel-lean, or near-stoichiometric. As expected from eq 2, only MnO was detected in the combustion products of the near-stoichiometric Mn/MnO_2 (40/60) mixture. At fuel-rich conditions, MnO and excess Mn were present, indicating that the Mn did not fully react, while for fuel-lean conditions, MnO and Mn_3O_4 were detected. All of the reactants and products (i.e., Mn, MnO, MnO_2, Mn_3O_4) have no known carcinogenic properties[29,30] and do not have the stringent regulations that are associated with hexavalent chromium and perchlorates.[7−9] In summary, the Mn/MnO_2 system is relatively benign compared to the current delay compositions that contain $BaCrO_4$, $PbCrO_4$, and $KClO_4$.

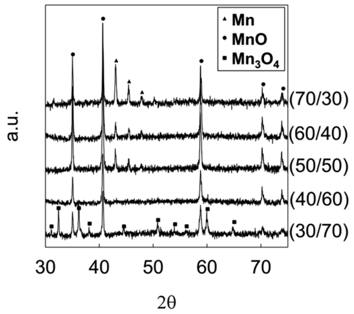

Figure 6. XRD analysis of Mn/MnO_2 combustion products from 4.7 mm Al channel experiments.

Effect of Accelerated Aging. It was previously documented that aging of the Mn-based delay system Mn/$BaCrO_4$/$PbCrO_4$ at 70 °C and 30% relative humidity led to performance degradation.[3] In contrast, the W/$BaCrO_4$/$KClO_4$/diatomaceous earth system did not show any performance degradation when aged under the same conditions.[3] However, it was not determined whether Mn oxidation or interaction of Mn with the oxidizers ($BaCrO_4$, $PbCrO_4$) led to the poor aging characteristics. There may still be potential aging concerns for the Mn/MnO_2 system. For example, growth of the Mn oxide layer (Mn_3O_4) could result in faster combustion velocities, while moisture absorption could result in slower combustion velocities when compositions are stored long-term.[17] In this study, three stoichiometries of Mn/MnO_2 were considered: 40, 50, and 60 wt % Mn. Aged premixed compositions and aged Mn/unaged MnO_2 compositions were assessed in 4.7 mm Al tubes every 2 weeks for 8 weeks to determine which constituent may cause a potential change in performance. As shown in Figure 7 (as well as Figures S2A and B, Supporting Information), combustion velocities remained within the standard deviation of the original velocity measurements of the unaged composition over a time period of 8 weeks. Additionally, Figure 8 shows the DSC/TGA analysis in an oxidizing environment (80/20 vol % Ar/O_2); no significant difference in active content was noted between unaged and aged Mn powder. A gradual weight gain above 250 °C is observed due to partial oxidation of Mn to form MnO. Exothermic peaks at 656 and 795 °C indicate the oxidation of Mn to MnO and MnO to Mn_2O_3, respectively. The endothermic reduction of Mn_2O_3 to Mn_3O_4 was observed at 928 °C and was accompanied by a small mass loss.[16] The endothermic phase change of α-Mn_3O_4 to β-Mn_3O_4 was observed at 1168 °C.[31] Since thermal analysis of the aged and unaged Mn produced similar DSC/TGA profiles while maintaining consistency with the documented thermal behavior of Mn/O_2, it appears that aging did not significantly alter the Mn.[16,31] Additionally, since aging according to standard NAVSEAINST 8020.5C did not result in altered combustion velocities (faster or slower), no coatings or inhibitors are likely necessary for long-term storage of this composition.[18]

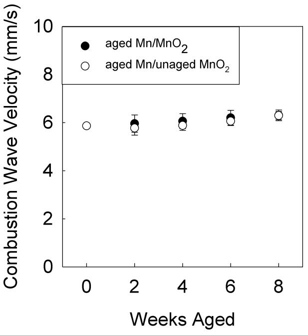

Figure 7. Combustion velocities of Mn/MnO_2 (40/60) as a function of aging duration. Open circles show data for aged Mn/unaged MnO_2 compositions, and closed circles show data for aged Mn/MnO_2 compositions.

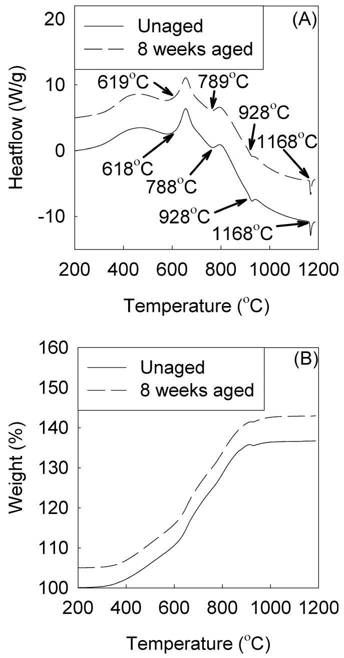

Figure 8. (A) DSC and (B) TGA scans of unaged and 8 weeks aged Mn at 20 °C min^{-1} with 80/20 vol % Ar/O_2 flow of 100 mL/min. For presentation clarity, the *y*-axis was staggered by 5 W/g and 5 wt %, respectively. The onset temperature of the exothermic event and the peak temperature of each endothermic event are labeled on the DSC plot.

CONCLUSION

In this study, Mn/MnO_2 was characterized as a potential replacement delay composition with aluminum microchannel combustion experiments, gas production experiments, ignition sensitivity assessments, combustion product analysis, and an accelerated aging study. The Mn/MnO_2 system was shown to propagate in 4.7 mm diameter aluminum microchannels similar to common delay housings. The attainable range of combustion velocities was affected by igniter type, while the combustion velocity depended primarily on stoichiometry, consistent with the measured combustion temperatures. For all stoichiometries, the Mn/MnO_2 system produced less gas than $W/BaCrO_4/KClO_4$/diatomaceous earth compositions, allowing it to be considered for use in sealed delay housings. An accelerated aging study according to NAVSEAINST 8020.5C at 70 °C and 30% relative humidity demonstrated that multiple stoichiometries maintain consistent performance over a period of 8 weeks. Additionally, near-stoichiometric Mn/MnO_2 was found to be insensitive to friction and ESD stimuli according to MIL-STD-1751A. The reactants and combustion products were found to only consist of unregulated compounds (i.e., Mn, MnO, MnO_2, Mn_3O_4) unlike current delay compositions, which contain $BaCrO_4$, $PbCrO_4$, and $KClO_4$. Overall, the Mn/MnO_2 system appears to be a suitable low gas-producing, nonsensitive, less toxic delay composition with combustion velocities in the range of 2.4−7.3 mm s^{-1} with good aging characteristics.

ASSOCIATED CONTENT

Ⓢ Supporting Information

Mn and MnO_2 size distribution data (Figure S1). Combustion velocities of (Figure S2A) Mn/MnO_2 (50/50) and (Figure S2B) Mn/MnO_2 (60/40) as a function of aging duration. Si/Bi_2O_3 and $W/BaCrO_4/KClO_4$/diatomaceous earth compositions mixing methods and the A1A composition mixing method. Additional combustion experiments in aluminum tubes and hand-held signal delay housings. Vendor information on reactant powders used in supplemental experiments (Table S1). Particle size distribution of Mn and MnO_2 powder used for supplemental experiments (Figure S3). Combustion experiment data in aluminum tubes and HHS delay housings (Table S2). This material is available free of charge via the Internet at http://pubs.acs.org.

AUTHOR INFORMATION

Corresponding Author

*E-mail: lori.groven@sdsmt.edu.

Notes

The authors declare no competing financial interest.

ACKNOWLEDGMENTS

This work was supported at Purdue University by the Armament Research, Development, and Engineering Center under Contract #TSS-242012-DK.

REFERENCES

(1) *Tungsten Delay Composition*. U.S. Military Specification MIL-T-23132A, 1972.

(2) *Manganese Delay Composition*. U.S. Military Specification MIL-M-21383A, 1976.

(3) Comyn, R. H. *Pyrotechnic Research at DOFL, Part II. Pyrotechnic Delays*; DTIC Accession Number: AD0273042; Technical Report for Diamond Ordnance Fuze Laboratories: Washington, DC, 1962.

(4) Zimmer-Galler, R. *The Combustion of Tungsten and Manganese Delay Systems*; DTIC Accession Number: AD0879499; Technical Report for Department of the Navy, Naval Ordnance Station: Indian Head, MD, 1970.

(5) Shachar, E.; Gany, A. Investigation of slow-propagation tungsten delay mixtures. *Propellants, Explos., Pyrotech.* **1997**, *22*, 207−211.

(6) Rose, J. E.; Valenta, F. J. *The Stability of Several Pyrotechnic Delay Compositions*; DTIC Accession Number: CPIAC-1998−2889; Technical Report for Indian Head Division, Naval Surface Warfare Center: Indian Head, MD, 1998.

(7) Sellers, K.; Weeks, K.; Alsop, W.; Clough, S. R.; Hoyt, M.; Pugh, B.; Robb, J. *Perchlorate: Environmental Problems and Solutions*; CRC Press Taylor & Francis Group: Boca Raton, FL, 2007.

(8) Guertin, J.; Jacobs, J. A.; Avakian, C. P. *Chromium (VI) Handbook*; CRC Press: Boca Raton, FL, 2004.

(9) *Toxicological Profile for Barium and Barium Compounds*; Technical Report for U.S. Agency for Toxic Substances and Disease Registry: Washington, DC, 2007.

(10) Miklaszewski, E. J.; Son, S. F.; Groven, L. J.; Poret, J. C.; Shaw, A. P.; Chen, G. In *Combustion Characteristics of Condensed Phase Reactions in Sub-Centimeter Geometries*, Proceedings of the 38th Internation Pyrotechnics Seminar, Denver, CO, June 10−15, 2012.

(11) Kalombo, L.; Del Fabbro, O.; Conradie, C.; Focke, W. W. Sb_6O_{13} and Bi_2O_3 as oxidants for Si in pyrotechnic time delay compositions. *Propellants, Explos., Pyrotech.* **2007**, *32*, 454−460.

(12) Poret, J. C.; Shaw, A. P.; Csernica, C. M.; Oyler, K. D.; Estes, D. P. Development and performance of the $W/Sb_2O_3/KIO_4$/lubricant pyrotechnic delay in the U.S. Army hand-held signal. *Propellants, Explos., Pyrotech.* **2013**, *38*, 35−40.

(13) Poret, J. C.; Shaw, A. P.; Groven, L. J.; Chen, G.; Oyler, K. D. In *Environmentally Benign Pyrotechnic Delays*, Proceeding of the 38th International Pyrotechnics Seminar, Denver, CO, June 10−15, 2012.

(14) Poret, J. C.; Shaw, A. P.; Csernica, C. M.; Oyler, K. D.; Vanatta, J. A.; Chen, G. Versatile boron carbide-based energetic time delay compositions. *ACS Sustainable Chem. Eng.* **2013**, *1*, 1333−1338.

(15) Miklaszewski, E. J.; Poret, J. C.; Shaw, A. P.; Son, S. F.; Groven, L. J. Ti/C-3Ni/Al as a replacement time delay composition. *Propellants, Explos., Pyrotech.* **2014**, *39*, 138−147.

(16) Swanepoel, D.; Fabbro, O. D.; Focke, W. W.; Conradie, C. Manganese as fuel in slow-burning pyrotechnic time delay compositions. *Propellants, Explos., Pyrotech.* **2010**, *35*, 105−113.

(17) Kappagantula, K. S.; Clark, B.; Pantoya, M. L. Flame propagation experiments of non-gas-generating nanocomposite reactive materials. *Energy Fuels* **2011**, *25*, 640−646.

(18) Peletski, C. *NAVSEAINST 8020.5C: Qualification and Final (TYPE) Qualification Procedures for Navy Explosives*; DTIC Accession Number: ADA509544; Technical Report for Naval Sea Systems Command: Arlington, VA, 2000.

(19) *Department of Defense Test Method Standard, Safety and Performance Tests for the Qualification of Explosives (High Exploxives, Propellants and Pyrotechnics)*; MIL-STD-1751A; Technical Report for Department of Defense, 2001.

(20) Puerta, M. C.; Valerga, P. Thermal decomposition of a natural manganese dioxide. *J. Chem. Educ.* **1990**, *67*, 344−346.

(21) Liu, B.; Thomas, P. S.; Ray, A. S.; Williams, R. P. The effect of sampling condition on the thermal decomposition of electrolytic manganese dioxide. *J. Therm. Anal. Calorim.* **2004**, *76*, 115−122.

(22) Desai, B. D.; Fernandes, J. B.; Dalal, V. N. K. Manganese dioxide − A review of a battery chemical. Part II. Solid state and electrochemical properties of manganese dioxides. *J. Power Sources* **1985**, *16*, 1−43.

(23) Bastea, S.; Fried, L. E.; Glaesemann, K. R.; Howard, W. M.; Kuo, I.-F.; Souers, P. C. *Cheetah 6.0 User Manual*; Technical Report for Lawrence Livermore National Laboratory, 2010.

(24) Zeldovitsch, J. B.; Frank-Kamenetzki, A. Theory of thermal propagation of flame. *Acta Physicochim. URS* **1938**, *9*, 341−350.

(25) Moore, J. J.; Feng, H. J. Combustion synthesis of advanced materials: Part I. Reaction Parameters. *Prog. Mater. Sci.* **1995**, *39*, 243−273.

(26) Conkling, J. A.; Mocella, C. *Chemistry of Pyrotechnics: Basic Principles and Theory*, Second ed.; Taylor and Francis Group, LLC: Boca Raton, FL, 2011.

(27) Rose, J. E. *Properties of Energetic Materials Used in Ordnance Devices*; 1HSP 89−288; September, 1990.

(28) Shaw, A. *Unpublished Tungsten Delay Sensitivity Data*. U.S. Army RDECOM-ARDEC: Picatinny Arsenal, NJ, 2013.

(29) *Manganese: TEACH Chemical Summary*; Technical Report for U.S. EPA: November, 2007.

(30) *Air Quality Guidelines for Europe*, Second ed.; WHO Regional Publications: Copenhagen, Denmark, 2000.

(31) Fetisov, V. B.; Fetisov, A. V.; Korchemkina, N. V.; Ovchinnikova, L. A.; Pastukhov, E. A.; Fishman, A. Y. Kinetics of redox processes in manganese oxides. *Dokl. Phys. Chem.* **2002**, *387*, 291−293.